

Exploring the LHC medium with electromagnetic probes

A. Marín¹ for the ALICE Collaboration

GSI, Planckstrasse 1, 64291 Darmstadt, Germany

Received: date / Revised version: date September 17, 2021

Abstract. Heavy-ion collisions will enter a new era with the start of the CERN Large Hadron Collider (LHC). A first short run with proton-proton collisions at the injection energy of 0.9 TeV will be followed by a longer one with pp collisions at 10 TeV. First Pb-Pb collisions at $\sqrt{s_{NN}}=5.5$ TeV will take place in 2009. Three experiments (ALICE, ATLAS, and CMS) will study both pp and Pb-Pb collisions. A selection of results showing the capabilities of the three experiments for the study of the LHC medium with electromagnetic probes is presented.

PACS. 25.75.-q Relativistic heavy-ion collisions – 13.85.Qk,25.75.Cj Photon, lepton

1 Introduction

With the startup of the CERN LHC heavy-ion collisions will enter a new era. With a center of mass energy of 5.5 TeV, about a factor 30 larger than the available energy at RHIC, matter will be produced in a new domain of high energy density (15 to 60 GeV/fm³) and high initial temperature (factor 3 to 5 higher than the critical Temperature, T_c). At high temperature and high energy density QCD calculations [1,2] predict a phase transition from hadron gas to quark gluon plasma (QGP) and chiral symmetry restoration. The expected time the system will spend in the QGP phase is of the order of 10 fm/c and it is expected to extend over a large volume. The cross sections of hard probes are increasing by large factors at LHC energies compared to RHIC or SPS [3]. Among the different observables photons and dileptons are particularly interesting because they would directly probe the high temperature and high density phase of these collisions. The pp runs will provide a test of pQCD as well as important reference data for heavy-ion runs. With the first heavy-ion run expected in 2009, the global event characteristics and bulk properties will be established, and hard probes measurements could be started.

2 Direct photon phenomenology at the LHC

There are different production mechanisms of photons in heavy-ion collisions. Direct photons are produced at leading order (LO) in quark gluon Compton scattering ($qg \rightarrow q\gamma$) and quark anti-quark annihilation ($q\bar{q} \rightarrow g\gamma$). The next-to-leading order (NLO) process is dominated by bremsstrahlung and fragmentation photons ($qg \rightarrow qq\gamma$). In addition, there are photons from the jet re-interaction in the medium and thermal photons from QGP and from the hot hadronic stage following the QGP. Direct photons have to be isolated from the main source of background photons, i.e. the decay of hadrons (mainly π^0 's and η 's) after the QGP phase.

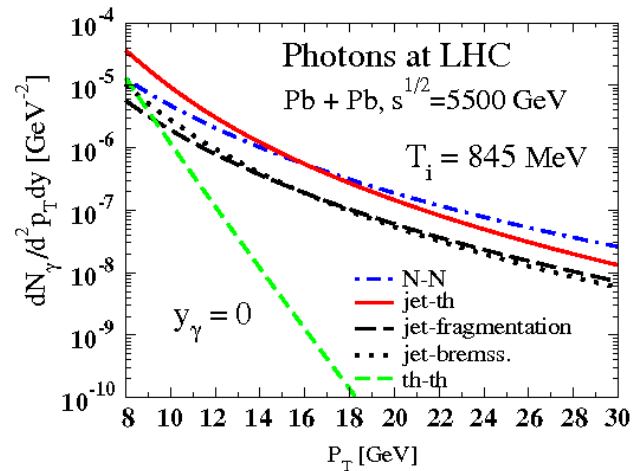


Fig. 1. Contributing sources of high- p_T photons at midrapidity in central Pb-Pb collisions at LHC from [4].

The different contributions to the direct photon spectrum for LHC energies as calculated by [4] is presented in Fig. 1. Other predictions are also available [5,6,7,8]. At RHIC γ 's from the parton scattering at LO were the dominant contribution for $p_T > 5$ GeV/c while at LHC jet-photon conversion in the plasma dominates between 8 and 14 GeV/c. Only for $p_T > 20$ GeV/c the hard NN scattering dominates. Although photons are more abundantly produced at LHC compared to RHIC (about a factor 10 larger), the ratio of direct photons to π^0 is smaller at LHC. The ratio is $\sim 10\%$ for a p_T of 20 GeV/c [9], thus a very good PID to distinguish between direct and decay photons would be essential.

Recently it has been proposed [10] that in order to distinguish between the different photon sources one can study their azimuthal anisotropy as function of p_T in conjunction with R_{AA} . A calculation for semicentral Pb-Pb collisions at LHC ener-

gies [11] predicts $v_2 = 0$ for initial production, positive for jet fragmentation and negative for jet photon conversion processes. Therefore, a negative v_2 together with $R_{AA} > 1$ will be an unambiguous signature of medium produced photons.

The high p_T photon measurement opens the possibility of studying the jet fragmentation function (FF) and its modification (redistribution of the parton energy inside the hadron jet) due to the medium effects in heavy-ion collisions by using the γ -jet channel. As the photon is not affected by final state interactions, its transverse energy (E_T) gives the energy of the jet before modification in the medium. This measurement would be complementary to jet reconstruction in the energy range from 20 GeV to 80 GeV [12], or above 75 GeV [13, 14].

3 ALICE, ATLAS and CMS as photon and dilepton detectors at the LHC

Three experiments will participate in the heavy-ion program at the CERN LHC. ALICE is the experiment devoted to the study of heavy-ion collisions [15, 16], and it will also participate in the pp running with an extensive physics program. ATLAS [17] and CMS [18] are experiments dedicated to study pp collisions although by now they also have a rich heavy-ion program [19, 20].

The ALICE detector (Fig. 2 top, Fig. 3 left) [15, 16] consist of central barrel detectors, a forward muon spectrometer and forward multiplicity and centrality detectors. The central barrel inside a large solenoid magnet with the field up to 0.5 T covers almost 2 units of pseudo-rapidity ($|\eta| < 0.9$). The charged particle tracking detectors are the ITS (Inner Tracking System) with three different silicon technologies (pixels, drift and strips), the TPC (Time Projection Chamber) main tracking system for charged particles, and the TRD (Transition Radiation Detector). All three tracking detectors are also used for particle identification (PID) by measuring ionization losses or transition radiation. The TOF (Time Of Flight) detector is used for PID in the intermediate momentum range (0.2 to 2.5 GeV/c). Three smaller single arm detectors complete the central barrel, the HMPID (High Momentum Particle Identification) detector that will extend the PID up to momenta of 4-5 GeV/c, the high resolution high granularity electromagnetic calorimeter PHOS (PHOTon Spectrometer) to measure photons and neutral mesons and the EMCAL (ElectroMagnetic CALorimeter) to improve the ALICE capabilities in the measurement of high energy jets and direct photons. At forward rapidities, ALICE triggers and detects muons using the muon spectrometer with tracking and trigger chambers in a 3 Tm magnetic field. ALICE has an excellent PID: $\pi/K/p$ identification up to 50 GeV/c and μ up to 100 GeV/c. The ALICE specific photon detectors are PHOS and the EMCAL. In addition, photons that convert in the detector material ($\gamma Z \rightarrow e^- e^+ Z$) can be detected by measuring the e^+ and e^- in the central barrel. This is a clean photon identification method, providing directional information used to reject non vertex background. The momentum resolution at low p_T using this method is better than electromagnetic calorimeters. The possibility of using a L1 TRD trigger [21] to make use of this method at high p_T is under investigation.

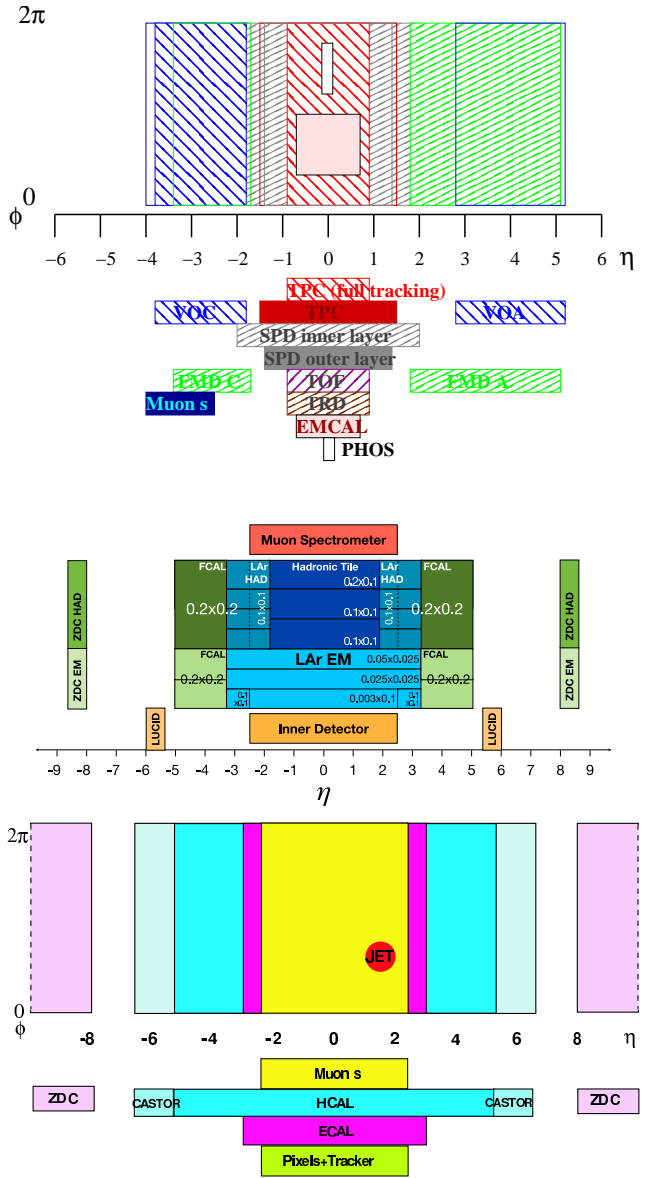


Fig. 2. ALICE (top), ATLAS (middle), and CMS (bottom) pseudorapidity and azimuthal coverage.

The ATLAS detector (Fig. 2 middle, Fig. 3 middle) [17, 19] has hermetic azimuthal coverage over a wide range in pseudo-rapidity. The unique feature of the ATLAS detector is its calorimetry, composed of several independent longitudinal sampling layers of electromagnetic and hadronic calorimetry with full azimuthal and $|\eta| < 5$ units coverage. Specially the Liquid Argon (LAr) electromagnetic calorimeter, which provides excellent energy and position information on electrons and photons. The inner tracking system within a 2T solenoidal field is equipped with silicon pixels, silicon strips and straw-tube transition-radiation tracker for reconstructing charged tracks within $|\eta| < 2.5$. A muon spectrometer ($|\eta| < 3$) is located within a toroidal field outside of the hadronic calorimeters.

The CMS detector (Fig. 2 bottom, Fig. 3 right) [18, 20] is also a hermetic detector with a large acceptance both for tracker and calorimetry. The CMS detector is a 22 m (length) x 15 m

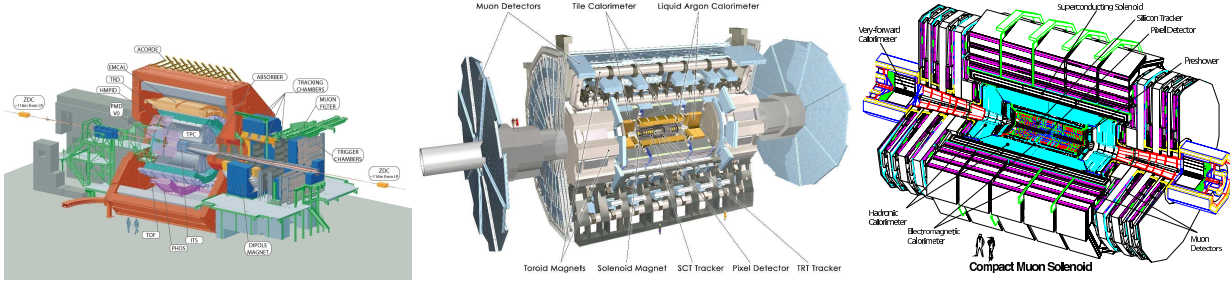


Fig. 3. Schematic layout of the ALICE (left), ATLAS (middle) and CMS (right) detectors.

Exp	ATLAS		CMS		ALICE		
Name	LAr Barrel	LArEndCap	ECAL(EB)	ECAL(EE)	PHOS	EMCAL	Barrel
Coverage	$0 < \eta < 1.4$ 2π	$1.4 < \eta < 3.2$ 2π	$0 < \eta < 1.5$ 2π	$1.5 < \eta < 3.$ 2π	$0 < \eta < 0.12$ 0.6π	$0 < \eta < 0.7$ 0.6π	$(0 < \eta < 0.9$ $2.\pi) \cdot 7X/X_0$
Granularity $\Delta\eta \times \Delta\phi$	0.003×0.100 0.025×0.025 0.025×0.025	0.025×0.100 0.025×0.025 0.025×0.025	0.017×0.017	0.017×0.017 to 0.05×0.05	0.004×0.004	0.014×0.014	$3 \cdot 10^{-4} \times 2 \cdot 10^{-4}$ resolution
Resolution	$10\% / \sqrt{E} \oplus$ 0.5%	$10\% / \sqrt{E} \oplus$ 0.5%	$2.7\% / \sqrt{E} \oplus$ 0.55%	$5.7\% / \sqrt{E} \oplus$ 0.55%	$1.3\% / \sqrt{E} \oplus$ 1.1%	$7\% / \sqrt{E} \oplus$ 1.5%	2% low pt 5% high pt

Table 1. Compilation of the photon detectors in the three LHC experiments with a brief description of their characteristics.

(diameter) detector featuring a 4 T solenoid surrounding central silicon pixel and micro-strip tracking detectors ($|\eta| < 2.4$) and electromagnetic ($|\eta| < 3$) and hadronic ($|\eta| < 5$) calorimeters. Muon detectors ($|\eta| < 2.4$) are embedded in the flux return iron yoke of the magnet. CMS detects leptons and both charged and neutral hadrons.

A compilation of the different photon detectors with their main characteristics in the three LHC experiments is presented in Table 1. PHOS and LAr (Barrel) have the best granularity.

4 Prompt photons and photon-tagged jets

To demonstrate the direct photon reconstruction capabilities ALICE has generated events using PYTHIA [22] triggered by prompt photons (γ -jet events) or π^0 (jet-jet events). To simulate Pb-Pb events, the pp events were merged with heavy-ion events generated by HIJING [23]. Prompt photons are selected in PHOS by applying cuts on the shape of the shower developed on the detector and isolation cuts [24, 25].

The spectrum of direct photons detected in PHOS for Pb-Pb collisions [24, 25] is shown in Fig. 4. An isolation cut of radius $R = \sqrt{\Delta\eta^2 + \Delta\phi^2} = 0.2$ and a p_T threshold of 2 GeV/c is used. The background rejection with the applied cuts is 1/14 for an efficiency of 50%. A sample of 2000 γ with $p_T > 20$ GeV/c is expected during one LHC running year.

The spectrum of prompt photons detected in 2 PHOS modules for pp collisions is presented in Fig. 5. An isolation cut with $R = 0.3$ and $\sum p_T < 2$ GeV/c has been used. A background rejection of 1/170 is obtained for an efficiency of 69%. A sample of 3000 γ with $p_T > 20$ GeV/c is expected during one LHC running year (10 pb^{-1}) [26].

As direct photons are not perturbed by the medium the fragmentation function of the recoiled jet can be measured using E_γ as the jet energy. The ratio of the measured fragmen-

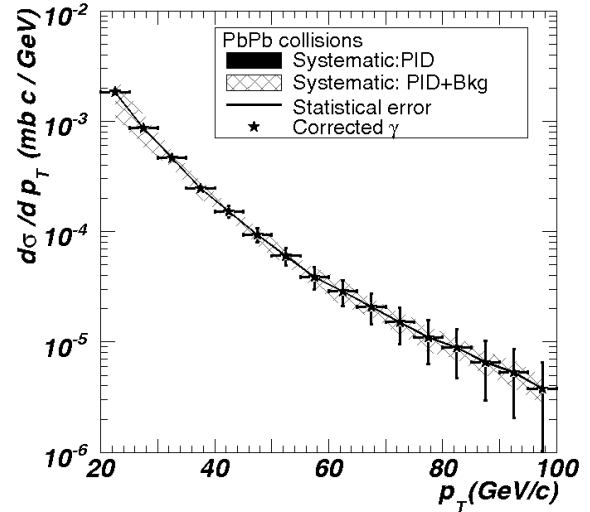


Fig. 4. Simulated prompt photon spectrum expected to be measured in ALICE during a LHC running year for Pb-Pb collisions with statistical (bars) and systematic (shaded band) errors.

tation functions for the two collision systems shows that for $E > 20$ GeV variations of R_{FF} larger than 5% in the range $0.1 < z = p_T/E_{jet} < 0.5$ can be measured, see Fig. 6.

The expected p_T reach of the prompt photon spectrum will be larger in ATLAS and in CMS compared to ALICE due to their larger acceptance.

Due to the fact that the ATLAS detector has very good granularity in the first layer, isolated photons give a very clear signal even in a heavy-ion background simulated using HIJING. The set of cuts based on shape of the signal and isolation cuts used for this study give an efficiency of about $\sim 60\%$ and a re-

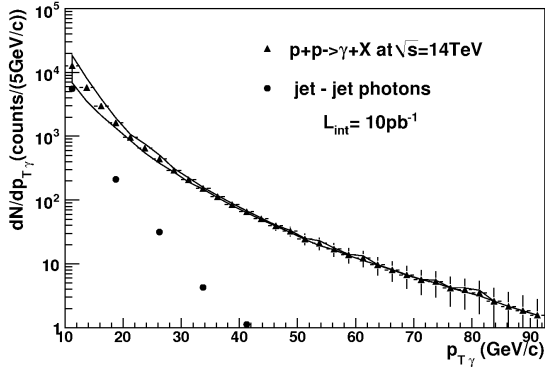


Fig. 5. Isolated photon spectrum that can be measured in ALICE with 2 PHOS modules in pp collisions at 14 TeV. The error bars are statistical errors. Systematic errors are given by the area around the data points.

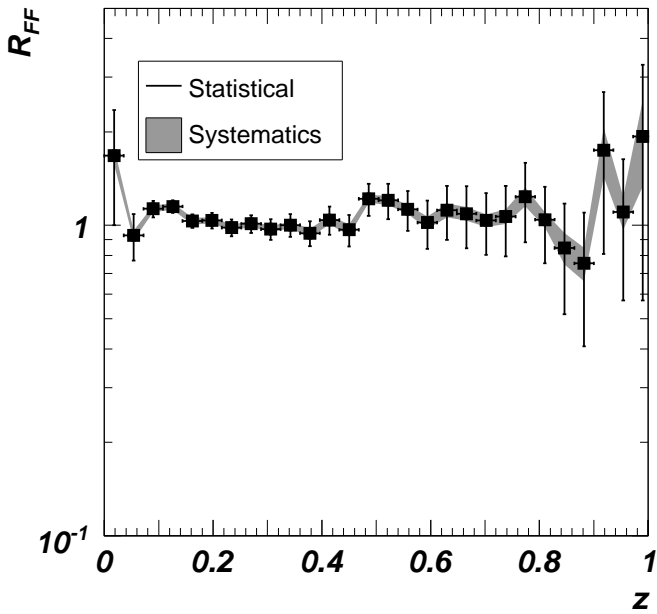


Fig. 6. Ratio of the fragmentation functions of γ -tagged jets with energy larger than 20 GeV for Pb-Pb collisions scaled to pp collisions detected in the central tracking system and EMCal. The shaded region represents the systematic error due to the contamination from jet-jet events.

jection factor of ~ 10 assuming $R_{AA}^h/R_{AA}^\gamma = 1$. The direct photon spectrum resulting from combining shape and isolation cuts is presented in Fig. 7 [14,27]. A sample of about 100K photons with $E > 30$ GeV and of about 10K with $E > 70$ GeV are expected for an integrated luminosity of 0.5 nb^{-1} .

CMS simulation studies are performed using PYQUEN [28] and PYTHIA to generate the prompt photons with and without jet quenching respectively, and HYDJET [29] to model the underlying heavy-ion event. The working point of the photon detection is set to 60% signal efficiency, leading to a background

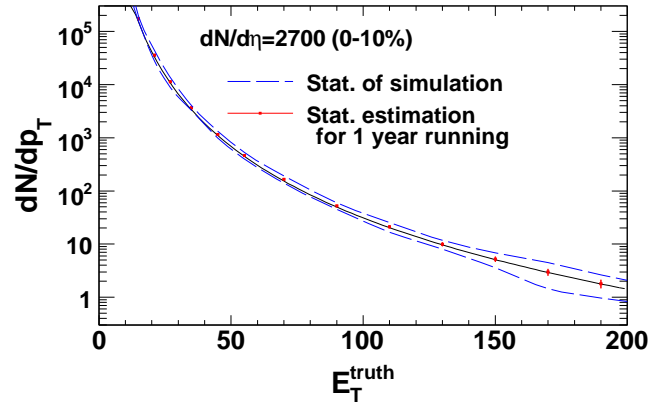


Fig. 7. Isolated photon spectrum as expected to be measured by the ATLAS detector in one LHC year running [27].

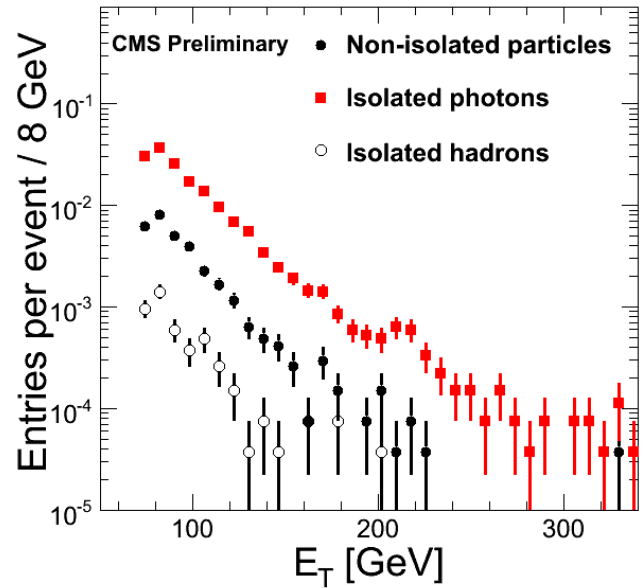


Fig. 8. Isolated photon spectrum as expected to be measured by CMS in one year of Pb-Pb collisions [13].

rejection of about 96.5%. The photon isolation and shape cuts improved S/B by a factor 15. A detailed description of the photon detection method can be found in [13]. The photon spectrum for an integrated luminosity of 0.5 nb^{-1} is shown in Fig. 8.

Isolated photons are associated with the back-to-back jet in order to reconstruct the fragmentation function. The ratio of the reconstructed fragmentation functions in quenched Pb-Pb and in pp is shown in Fig. 9. CMS obtains high significance for ξ between 0.2 and 5 for E_γ larger than 70 GeV (Fig. 9).

In addition to the γ -tagged jet measurement, jets can also be tagged with a virtual photon or a Z^0 . This method is free from the bias of the isolation cut that is applied in γ -tagged jets. A detailed study for the CMS detector is presented in [20,30].

5 Low mass dileptons

The measurement of direct photons at low p_T is usually performed on a statistical basis, namely subtracting the decay pho-

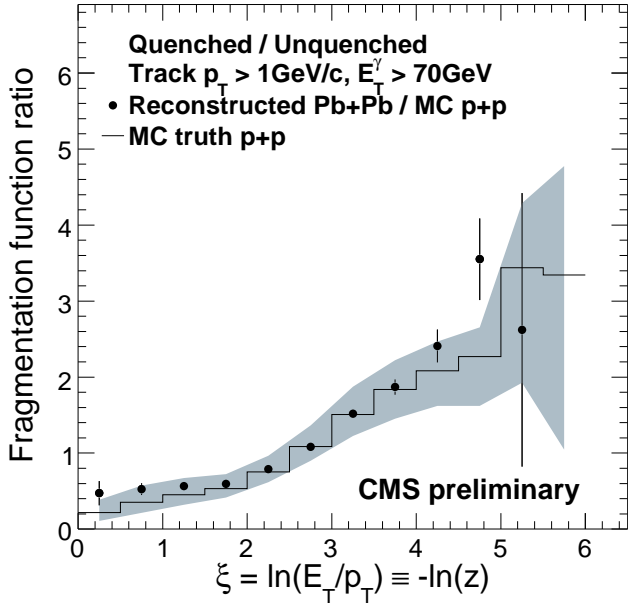


Fig. 9. Ratio of reconstructed (symbols) and MC truth (line) quenched fragmentation function over unquenched MC truth in CMS. The estimated systematic error is given by the shared band [13].

tons from all detected photons [31]. The difficulty of this method comes from the large background due to the decay photons. To overcome the background problem it has been proposed to consider instead the emission of virtual photons (lepton pairs). This method was used at CERN ISR to set a limit on direct photon production [32]. The invariant mass distribution of Dalitz decay pairs as well as of virtual photons is given by the Knoll-Wada formula [33].

Beyond the mass of the π^0 , only the η mesons contributes. As most of the γ 's come from π^0 decays, the signal to background ratio for direct photon signal improves considerably for $m_{ee} > m_{\pi^0}$. This method also benefits from the excellent mass resolution at low invariant mass and from the low conversion probability in the case of ALICE ($\sim 7\%$). For ATLAS and for CMS, where the conversion probability is higher ($\sim 20\%$, $\sim 30\%$), it would be more difficult to apply this method.

This method has also been used recently by PHENIX to measure direct photons in pp and Au+Au [34]. While the yield is consistent with NLO pQCD calculations in pp collisions, in AuAu collisions the data are larger than calculations for $p_T < 3.5$ GeV/c.

Theoretically, the rate of production of a dilepton pair in a finite mass range is given by [35]

$$\frac{d\sigma^{e^+e^-}}{dp_T dy} = C_{e^+e^-} \alpha \frac{d\sigma^\gamma}{dp_T dy} \quad (1)$$

where $C_{e^+e^-} \sim 0.3$ for $0.2 \text{ GeV}/c^2 < M_{e^+e^-} < 0.6 \text{ GeV}/c^2$ valid in the range $2 \text{ GeV}/c < p_T < 100 \text{ GeV}/c$. The expected yield of virtual photons calculated taking into account Eq 1 and the pQCD rate for a LHC running year is shown in Fig. 10. Thermal photons are supposed to be the dominating contribution below $p_T \sim 5 \text{ GeV}/c$ [5, 6, 7], therefore the dilepton yield is probably underestimated. Points for p_T below $2 \text{ GeV}/c$ should be

taken with some caution, as this method assumes that the mass of the dilepton pair is negligible compared to the p_T and the validity of Eq. 1. The electron pairs are detected and identified by the ALICE central tracking system (TPC and TRD).

6 Conclusions

The LHC machine and the experiments are finally a reality. We have shown that the three experiments are equipped with very good photon and dilepton detectors that will allow the measurement of electromagnetic probes at LHC energies from low to very high p_T . The low mass dilepton measurement will extend the direct photon spectrum to lower p_T . The jet fragmentation function and its modification due to the medium effects in heavy-ion collisions will be study using γ tagged jets. The ALICE, ATLAS and CMS experiments will provide independent and complementary results, that will be essential to understand this new system.

Acknowledgements. I would like to express my gratitude to the organizers of the 3rd International Conference on Hard and Electromagnetic Probes in High Energy Nuclear Collisions and the ALICE management for the invitation to speak in A Toxa. I would like also to thank the ALICE, the ATLAS and the CMS Collaborations for providing the material for this talk and for useful discussions. The author wishes to acknowledge the financial support received from GSI and from the German BMBF.

References

1. F. Karsch, hep-lat/0106019.
2. M. Cheng *et al.*, Phys. Rev. D 77, 014511 (2008)
3. C. Fabjan *et al.*, proceedings of Quark Matter Conference 2008
4. S. Turbide *et al.*, Phys. Rev. C 72, 014906 (2005)
5. R.J. Fries *et al.*, Phys. Rev. Lett. 90, 132301 (2003)
6. S. Turbide *et al.*, Phys. Rev. C 69, 014903 (2004)
7. F. Arleo *et al.*, nucl-th/0707.2357v2.
8. N. Armesto *et al.*, J. Phys. G: Nucl. Part. Phys. 35, 054001 (2008)
9. F. Arleo *et al.*, LHC CERN Yellow Report 2004-009. hep-ph/0311131
10. S. Turbide *et al.*, Phys. Rev. Lett. 96, 032303 (2006)
11. W. Liu, R.J. Fries, nucl-th/0801.0453.
12. C. Klein-Boesing *et al.* (ALICE Collaboration), these proceedings.
13. C. Loizides *et al.*, (CMS Collaboration), arXiv 0804.3679v1, nucl-ex, proceedings of Quark Matter Conference 2008
14. N. Grau *et al.*, (ATLAS Collaboration), arXiv:0805.4656v1, nucl-ex
15. ALICE Collaboration *et al.*, J. Phys. G: Nucl. Part. Phys. 30, 1517 (2004)
16. ALICE Collaboration *et al.*, J. Phys. G: Nucl. Part. Phys. 32, 1295 (2006)
17. ATLAS Collaboration, ATLAS Technical Design Report, vol 1 CERN/LHCC 1999-14, vol 2 CERN/LHCC 1999-15
18. CMS Collaboration *et al.*, The CMS Physics Technical Design Report, Volume 1, CERN/LHCC 2006-001
19. ATLAS Collaboration, Letter of Intent, Report CERN/LHCC/2004-009

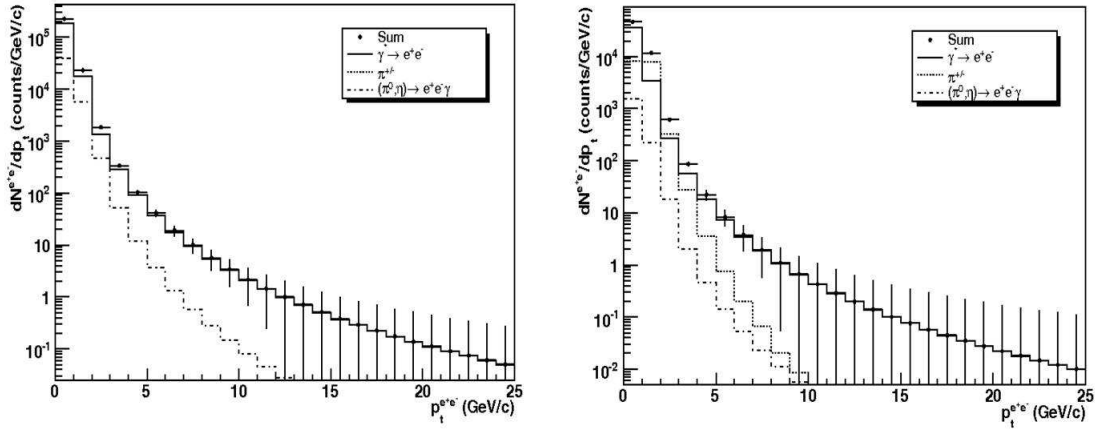


Fig. 10. Virtual photon spectrum reconstructed from the measurement of electron pairs with mass on the range 0.2 to 0.6 GeV/c² in pp at $\sqrt{s}=5.5$ TeV (left) and in central Pb-Pb collisions (right) at $\sqrt{s_{NN}}=5.5$ TeV.

20. D.G. d'Enterria *et al* (CMS Collaboration), J. Phys. G: Nucl. Part. Phys. 34, 2307 (2007)
21. ALICE Collaboration *al*, TRD Technical Design Report, CERN/LHCC 2001-021
22. T. Sjostrand *et al*, Comp. Phys. Comm. 135, 238 (2001)
23. X.N. Wang, N. Gyulassy, Phys. Rev. D 44 (1991) 3501; M. Gyulassy, X.N. Wang, Comp. Phys. Comm. 83, 307 (1994)
24. G. Conesa *et al*, Nucl. Instr. and Meth. A 580, 1446 (2007)
25. G. Conesa *et al*, Nucl. Instr. and Meth. A 585, 28 (2008)
26. Y. Mao *et al*, (ALICE Collaboration), proceedings of Quark Matter Conference 2008. ALICE-INT (2007) 021
27. B. A. Cole *et al*, (ATLAS Collaboration), these proceedings
28. I. P. Lokhtin and A. M. Snigirev, Eur. Phys J. C 45, 211 (2006) [PYQUEN v1.2 is used]
29. I. P. Lokhtin and A. M. Snigirev, ArXiv:hep-ph/0312204 [HYD-JET v1.2 is used]
30. C. J. Kunde *et al*, these proceedings
31. D. Peressounko *et al*, (ALICE Collaboration), these proceedings
32. J. H. Cobb *et al*, Phys. Lett. B 78, 519 (1978)
33. N. M. Knoll and W. Wada, Phys. Rev. 98, 1355 (1955)
34. A. Adare *et al*, (PHENIX Collaboration) arXiv:0804.4168v1 (nucl-ex).
35. P. Aurenche *et al*, Phys. Lett. B 209, 375 (1988)